A Discrete Tomography Approach to PET Reconstruction

Myriam Servières, JeanPierre Guédon, and Nicolas Normand
IRCCyN - UMR CNRS 6597, Image & Video Communication,
École polytechnique de l'Université de Nantes
La Chantrerie, BP 50609, 44306 Nantes Cedex 3
Email: {myriam.servieres, jean-pierre.guedon, nicolas.normand}@polytech.univ-nantes.fr

***Abstract*— In this paper, the popular FBP algorithm is revisited using discrete tomography. More precisely, our version of the discrete exact Radon (inverse) transform called the Mojette transform is used to model the discrete geometry into which are mapped the initial data. This allows for an exact backprojector definition that is then mixed with the spline-FBP algorithm [2] to produce a novel Mojette-FBP scheme. Adequation to practical geometries used in 3D medical imaging as 3D-PET is presented.**

I. Introduction

The Radon Transform [10] represents an interesting problem to discretize because of its ill-posed nature [2]. Discrete operators start to emerge in the tomographic reconstruction field. Until recently, the field of discrete tomography was working onto the reconstruction problem with pure mathematics objectives. Linking discrete tomography with medical tomography is an ongoing process [4][8]. In this paper, we are willing to give new discrete and consistent tools to the tomographic reconstruction. First, the geometry of acquisition can be modeled using discrete angles as was done by M. Katz [7]. Second, the corresponding discrete Radon transform will be derived properly using the Mojette transform that has been studied in our group for some years [9]. Third, the stability of the obtained exact backprojector and the instability of the scheme in presence of noise lead to derive a new Mojette FBP scheme that is finally presented.

II. A Linear Discrete Exact Radon Transform: the Mojette operator

The splines spaces (since they represent a reproducing kernel of Sobolev spaces) will be the choice to project the discrete Radon solutions issued from our derived schemes. Because of the recurrent relationships between spline orders, only splines of order 0 are considered here without loss of generality [6]. In other words, the formulation for a continuous function $f(x,y)$ from samples $f(k,l)$ is given by:

$$f_0(x,y) = \sum_{k=-\infty}^{+\infty} \sum_{l=-\infty}^{+\infty} f(k,l)\beta_0(x-k)\beta_0(y-l) \qquad (1)$$

where function $\beta_0(x)$ is the step function of unitary length. The Radon transform is given in its continuous mode by:

$$\begin{aligned} proj(t,\theta) &= \mathbf{R}f(x,y) \\ &= \int_{-\infty}^{+\infty}\int_{-\infty}^{+\infty} f(x,y)\delta(t + x\sin\theta - y\cos\theta)\,dxdy \end{aligned} \qquad (2)$$

Using Eq. 2 to project the grid used in Eq. 1 leads to the major choice of only using discrete angles of the form $\theta = \mathrm{atan}\frac{q}{p}$ where p and q are integers (moreover, a single representant of the angle class is kept by restricting p and q to be prime together and q to be positive). Effectively, when jointly using such an angle with the projection sampling (were b is called a bin) leads to a regular lattice with keeping all pixels centers onto projection bins. In this case, Eq. 2 is reduced to [3] :

$$\begin{aligned} proj(b,p,q) &= M_\delta f(k,l) \\ &= \sum_{k=-\infty}^{+\infty}\sum_{l=-\infty}^{+\infty} f(k,l)\Delta(b+qk-pl) \end{aligned} \qquad (3)$$

where $\Delta(b) = \begin{cases} 0 \text{ if } b \neq 0 \\ 1 \text{ if } b = 0 \end{cases}$ is the discrete Kronecker symbol. Eq. 3 defines the Mojette transform operator (see Fig. 1).

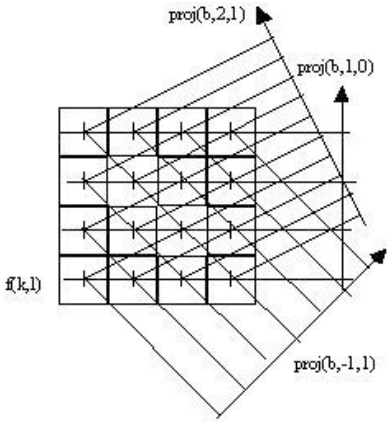

Fig. 1. Mojette projection of a 4×4 image with projection directions $(p,q) = \{(1,0),(-1,1),(2,1)\}$

The 2D Mojette transform defined in Eq. 3 has some interesting properties. Linearity and shift-invarianceness of the Radon transform are kept because both angular and projection samplings are realized in an adequate manner. Reconstruction can be exactly performed with a finite number of angles [9]. Notice that Eq. 3 could also be written as :

$$proj(b,p,q) = M_\delta f(k,l) = \sum_{k=-\infty}^{+\infty}\sum_{l=-\infty}^{+\infty} f(k,l)\Delta\left(b - P_{21}\begin{pmatrix} k \\ l \end{pmatrix}\right) \quad (4)$$

with $P_{21} = (-q\ p)$.

This gives a simple way to derive the 3D Mojette operator transform for a convex volume $f(k,l,m)$ with the discrete projection planes indexed by vector $B^T = (b_1, b_2)$ at given angle (p,q,r) with $\gcd(p,q,r) = 1$ by :

$$proj(B,p,q,r) = M_\delta f(k,l,m) = \sum_{k=-\infty}^{+\infty}\sum_{l=-\infty}^{+\infty}\sum_{m=-\infty}^{+\infty} f(k,l,m)\Delta\left(B - P_{32}\begin{pmatrix} k \\ l \\ m \end{pmatrix}\right) \quad (5)$$

with $P_{32} = \begin{pmatrix} 1 & 0 & \frac{-p}{r} \\ 0 & 1 & \frac{-q}{r} \end{pmatrix}$ when $r \neq 0$.

The main characteristic of the Mojette transform lies in the sampling (first presented in [7]). Another way of seeing this is to say that the linear system expressed in Eq. 3 is exactly invertible because of the sampling. From a rectangular image $Q \times P$, this matrix inversion must be possible to perform an inverse mojette transform, i.e. a minimum number of projections is required. For the rectangular shape, the Katz criterion allows reconstruction if:

$$P \leq \sum_{i=1}^{I} |p_i| \text{ or } Q \leq \sum_{i=1}^{I} |q_i| \quad (6)$$

where I is the number of projections.

In other words, the reconstruction does not depend directly on the number of bins but is first related to the number of projections. These reconstruction conditions have been generalized for any convex shape using a simple morphological tool : a two pixel structuring element that depicts a discrete direction [9].

The inverse Mojette operator is also defined in a specific way. Instead of a matrix inversion (which is possible), the operator only proceeds by finding at each iteration a discrete corner of the shape under reconstruction which is the only projected pixel onto a bin : the bin value is exactly backprojected and all projections are updated. The algorithm complexity of both the direct and inverse Mojette transform is $O(IN)$ where N is the number of pixels.

So far, the defined Mojette transform does not act onto the spline spaces. Fortunately, a generalization of the operator to any spline order is simple as shown in [3] and connect to the FBP derivation made in [2]. The physical projection expressed in Eq. 2 means that the integration line giving the bin value could be interpreted as either discrete (jumps between pixel centers) or continuous. Designing a projection operator M_0 as in Eq. 3 which will sum the whole line is simply adding a convolution (in the image plane) with a spline 0 order as expressed in Eq. 1.

$$proj_0(b,p,q) = M_0 f(k,l) = \sum_{k=-\infty}^{+\infty}\sum_{l=-\infty}^{+\infty} f(k,l)trapeze(b+qk-pl) \quad (7)$$

Again, as demonstrated in [3], this corresponds to convolve the discrete Mojette projection (this result is only valid for (p,q)-angle) with a discrete trapezoidal filter. The latter can be roughly expressed as the convolution of two series of unitary values of respective lengths p and q.

III. Mojette and PET geometries

The geometry of PET acquisition devices can be modelled by the discrete geometry derived from the Mojette discrete space. As a matter of fact, each disintegration captured by a pair of detectors corresponds to a solid angle defined by the length between detectors and the size of an elementary detector. In other words, a single photon count does not corresponds to a single angle. So it can be assigned to any angle lying into this solid angle. Specifically, we propose to compute a discrete angle indexed by (p,q,r) to each detection and to increment the corresponding Mojette bin onto the discrete plane.

Mojette discrete geometry is used for 3D PET reconstruction by the choice of the (p,q,r) angles set for the whole detection set which depends on the desired resolution for reconstruction. This has been shown in a slight different context [2] for SPECT acquisition. From the Mojette point of view, it becomes clear that pixel and bin resolution are strongly related through the angle direction. The set of planes allowing (according to Katz'criterion) a given resolution is fulfilled with this algorithm. Acting this way, the approximation between original and discrete data is minimized.

Nevertheless, two main problems are still to be addressed. First, data are noisy, whereas the standard inverse Mojette algorithm does obviously a poor job in this case since errors will propagate and increase from the corners to the center of the image. This has led to use this instability for a watermarking scheme where the mark acts as a noise added onto Mojette projections [1]. This main concern can be overcome by the use of a multiresolution algorithm that will evaluate the noise and use the signal properties at each step. Second, there are missing data on PET projection plane and again the standard inverse Mojette reconstruction can not be simply implemented.

The other way to avoid these problems is to use a direct reconstruction method which split the inverse Mojette operator into a filter onto the projections and an exact backprojector.This is the FBP-Mojette algorithm now presented.

IV. The FBP-Mojette algorithm

A. Theory

Following the discrete approach of the PET reconstruction problem will lead to design an exact discrete filter which

has to be consistent with the discrete set of angles obtained from the acquisition model. This induces a complicated design corresponding to the notion of a an equivalent discrete Ramp in the Z transform domain. However, a filter derived from a corresponding continuous version can be used. In [3] the spline Mojette operators have been presented. In particular, the Haar Mojette operator that corresponds to model the bin value by the entire continuous line summation (not the discrete line as the Dirac Mojette operator) can be used. The continuous exact Haar-FBP filter was derived in [2] and its expression in the Fourier domain is given by:

$$K_0(\nu,\theta) \quad = \quad \pi\,|\nu|\,\mathrm{sinc}(\nu\cos\theta)\mathrm{sinc}(\nu\sin\theta) \tag{8}$$

where the apodisation function corresponds to the projection of the filter onto the spline of order 0 space. The pixel size is 1×1

The inverse fourier transform of Eq. 8 was derived as

$$k_0(t,\theta) = \frac{1}{\pi\sin(2\theta)}\ln\left|\frac{t^2-(\frac{1+\sin(2\theta)}{4})}{t^2-(\frac{1-\sin(2\theta)}{4})}\right| \tag{9}$$

for $t \neq 0$ and $\theta \in]0, \frac{\pi}{4}]$ and $k_0(t,0) = \frac{-1}{\pi}\frac{2}{4t^2-1}$.

Discretizing with Mojette angles ($\tan\theta = \frac{q}{p}$) with the projection sampling $t = \frac{b}{\sqrt{p^2+q^2}}$ leads to:

$$k_0(b,p,q) = \frac{p^2+q^2}{2\pi pq}\ln\left|\frac{b^2-(\frac{p+q}{2})^2}{b^2-(\frac{p-q}{2})^2}\right| \tag{10}$$

for $b \neq 0$ and $(p,q) \neq (1,0)$ and $k_0(b,1,0) = \frac{-1}{\pi}\frac{2}{4b^2-1}$.

Notice that this filter can not be implemented in a straightforward manner. It exhibits discontinuities at the points where the projection of the pixel (which is described by a trapezoidal shape) is continuous but not differentiable. The Ramp filter acting as a derivation operator, the values at these points have to be computed using the Dirichlet condition.

For a single angle (p,q) the discrete backprojector is defined by:

$$\begin{aligned}\tilde{f}(k,l) &= M^* proj(b,p,q) \\ &= \sum_i\sum_j \delta(k-i)\delta(l-j) \\ &\quad \sum_b proj(b,p,q)\Delta(b+qi-pj)\end{aligned} \tag{11}$$

Lemma: The Mojette dual operator M^* corresponds to an exact discrete backprojector operator. (See Fig. 2) The demonstration is straighforward by applying the Mojette operator onto Eq. 11 :

$$\begin{aligned}&MM^* proj(b,p,q) = \\ &\sum_k\sum_l\sum_i\sum_j \delta(k-i)\delta(l-j)\Delta(b+qi-pj) \\ &\quad \sum_b proj(b,p,q)\Delta(b+qk-pl)\end{aligned} \tag{12}$$

leading to :

$$\begin{aligned}&MM^* proj(b,p,q) \\ &= \sum_b proj(b,p,q)\sum_i\sum_j \Delta(b+qi-pj)\end{aligned} \tag{13}$$

Then, using a Mojette angle sampling allows to back-project onto pixel centres without any interpolation. In other words, the FBP-Mojette operator is exact for the filter when an infinite number of angles is used and exact for the backprojection of these filtered angles.

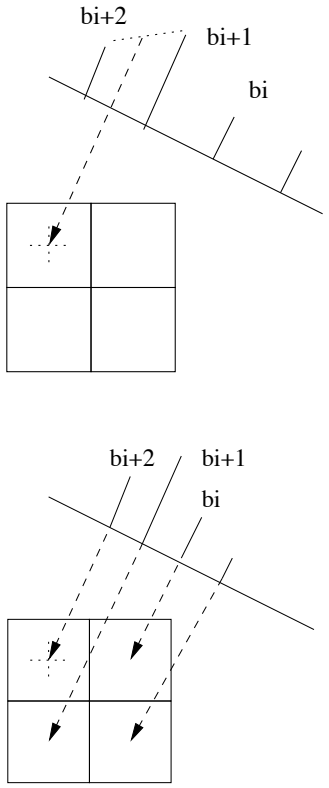

Fig. 2. (a) Interpolation onto the projection in order to backproject the right value at the corresponding centre of the pixel, (b) Exact Mojette backprojector.

B. Implementation

We performed the implementation of the Mojette FBP algorithm. The considered test image is only composed of a centered square box with unitary value of 15 pixel width onto a null background. An additional half-valued border was added with quarter-valued corners to ensure a Dirichlet condition. The image size was 128×128.

Projections angles were carefully computed as follow. The Farey series of order 128 was used to generate a very high (20088) number of projections. Then, a subset of 128 projections was chosen among the 20088 projections by taking values close to the regular angular sampling. This computation was mandatory to obtain a gracefully distributed set of discrete angles. Indeed, choosing a Farey series of lower order leads

to unequal angular sampling that will result into degradation of the FBP Mojette reconstruction. The projection operator was simply designed by applying the Dirac-projector M (Eq. 3) without the smoothing by the trapezoidal window (which would be necessary if the classical projection operator would have to be simulated). Thus the spatial filter k_0 was convolved with the projection and the backprojector M^* applied. Fig. 3 shows the reconstruction for the set of 128 gracefully distributed angles.

We measure the reconstruction error with the *normalised root mean squared distance measure* MRNSDM and the *normalised mean absolute distance measure* NMADM [5]. A large difference in a few places cause the NRNSDM to be large. The NMADM emphasise the importance of a lot of small errors rather than a few large errors. They are defined by:

$$MRNSDM = \left(\frac{\sum_{k=1}^{N} \sum_{l=1}^{N} (p_{k,l} - \tilde{p}_{k,l})^2}{\sum_{k=1}^{N} \sum_{l=1}^{N} (p_{k,l} - \bar{p})^2} \right)^{\frac{1}{2}} \quad (14)$$

$$NMADM = \frac{\sum_{k=1}^{N} \sum_{l=1}^{N} |p_{k,l} - \tilde{p}_{k,l}|}{\sum_{k=1}^{N} \sum_{l=1}^{N} |p_{k,l}|} \quad (15)$$

with $p_{k,l}$ with $k, l \in [1..N]$ original image's pixels, $\tilde{p}_{k,l}$ with $k, l \in [1..N]$ reconstruct image's pixels and $\bar{p}$ pixels mean in original image.

Results are very promising. It has to be noticed that the rule of thumb to get the appropriate sampling (projection sampling compared to image sampling, number of projections) given in [2] seems not respected here. In fact, the present situation is highly difficult to assess because the sampling path onto the projection is angle-dependent. For instance, the angle $\theta = 0$ leads to a convolution filter without oversampling (thus misleading the Dirichlet condition). This explains the obtained artefacts at $\theta = 0$ or $\theta = \frac{\pi}{2}$.

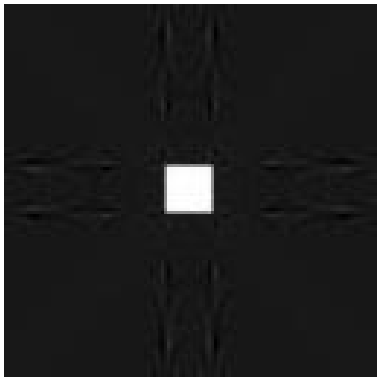

Fig. 3. Image reconstruction with 128 gracefully distributed angles. MRNSDM = 0.000814, NMADM = 0.313296

V. Conclusion

In this paper a new version of the classical FBP algorithm has been presented. This FBP-Mojette algorithm is perfectly suited for a discrete version of the Radon transform. It has to be noticed that the proposed algorithm gives an exact backprojector for the dual of the projection operator. This leads to an implementation without approximations for the backprojector. Therefore, the approximated part of the reconstruction is the finite number of projections.

The next work in this direction will be to define the equivalent filter corresponding to a finite number of projections. This will allowed to connect with the inverse Mojette operator.

References

[1] F. Autrusseau, JP. Guédon, and Yves Bizais. Mojette cryptomarking algorithm for medical images. In *Medical Imaging 2003*, pages 958–965, Febuary 2003.

[2] JeanPierre Guédon and Yves Bizais. Bandlimited and haar filtered back-projection reconstuction. *IEEE transaction on medical imaging*, 13(3):430–440, September 1994.

[3] JeanPierre Guédon and Nicolas Normand. Spline mojette transform. application in tomography and communication. *EUSIPCO*, 2002.

[4] G Herman and A Kuba. *Discrete tomography, Foundations, algorithms and applications (Applied and numerical harmonics analysis series)*. Springer-Verlag, 1999.

[5] Gabor T. Herman. *Image Reconstruction From Projections*. Computer Science and Applied Mathematics,The Fundamentals of Computerized Tomography, academic press edition, 1980.

[6] S. Horbelt, M. Unser, and JP Guédon. Spline discretization of the radon transform. Technical report, EPFL, Internal report, 1998.

[7] M. Katz. *Questions of Uniqueness and Resolution in Reconstruction from projections*, volume 26. Springer-Verlag, 1979.

[8] A. Kuba. Reconstruction in different classes of 2d discrete sets. *Lecture Notes on Computer Science*, pages 153–163, 1999.

[9] Nicolas Normand and JeanPierre Guédon. La transformée mojette : une représentation redondante pour l'image. *Comptes Rendu de l'Académie des Sciences, Informatique Théorique*, 325, 1997.

[10] J. Radon. Uber die bestimming von functionen durch ihre integralwerte langs gewisser mannigfaltigkeiten. *Berichte Sashsische Academie der Wissenshaften, math. - phys*, 69:262–267, 1917.